Global features of gyrokinetic simulations with sources

L Villard[1], E Lanti[1], N Ohana[1], A Scheinberg[1], B F McMillan[2], S Brunner[1], G Merlo[3], J Dominski[4]

[1] Ecole Polytechnique Fédérale de Lausanne, Swiss Plasma Center, Switzerland
[2] Center for Fusion, Space and Astrophysics, University of Warwick, United Kingdom
[3] University of California Los Angeles, CA, USA
[4] Princeton Plasma Physics Laboratory, NJ, USA

1. Summary

- Collisionless gyrokinetics (GK). In the absence of dissipation, statistical steady state can never be reached [Krommes PoP 2009]. Indefinite filamentation of phase space, unrestricted entropy growth while low-order moments may seem to have saturated ("entropy paradox").
- GK codes include some form of (unphysical) dissipative 'regularization' mechanism, $\Rightarrow$ smoothing of phase space. Lagrangian (PIC): various 'noise control' methods. Eulerian (grid-based): (explicit) hyperdiffusion term and (implicit) dissipation due to finite grid size.
- **Aim of this paper: ensure the noise control method provides enough phase space smoothing without a large unphysical impact on the physics of interest.**
- In addition, source terms are typically added for maintaining, or driving the system in a quasi-steady state with gradients above marginality. **Conserving or not conserving certain moments will be shown to have a *measurable* effect on transport, parallel and $E \times B$ flows, and avalanche behaviour.**

Global features observed in TCV experiments: coherent oscillations, $f < f_{GAM}$, large radial extension, radially propagating [deMeijere PPCF 2014]

- Global GK simulations with ORB5 [Vernay PhD 2014] and GENE [Merlo PPCF 2017]: similar feature, some agreement with experiment. **Here: Conserving or non-conserving source terms has an effect on the presence of absence of this feature.**
- These GAM-like features are in fact avalanches that propagate radially [McMillan PoP 2009, Candy 2003, Görler PoP 2011, Dif-Pradalier PRE 2010] non-resonantly driven by turbulence.

2. Global gyrokinetic model and sources

$$\frac{\partial f_\sigma}{\partial t} + \dot{\mathbf{R}} \cdot \frac{\partial f_\sigma}{\partial \mathbf{R}} + \dot{v}_\parallel \frac{\partial f_\sigma}{\partial v_\parallel} = \sum_{\sigma'} C(f_\sigma, f_{\sigma'}) + S(f_\sigma)\ , \qquad (1)$$

In this paper: collisionless ($C = 0$), electrostatic, adiabatic electrons.
Hybrid electron model: see [Lanti, EFTC 2017]
Solved using the ORB5 code: global, PIC

Source terms, flux-averaged momentum conservations [McMillan PoP 2008]
$S = -\gamma_K \delta f + S_{\rm corr}$, with $S_{\rm corr}$ such that

$$\left\langle \int \mathrm{d}\vec{v} M_i (\gamma_K \delta f + S_{\rm corr}) \right\rangle = 0, \text{ with } M_i = [1, v_\parallel, (v_\parallel/B - (v_\parallel/B)_b), v^2/2 + \mu B] \qquad (2)$$

M_3 preserves phase space structure of the undamped Rosenbluth-Hinton $E \times B$ Zonal Flow (ZF) residual (long radial wavelength limit) [McMillan PoP 2008] (subscript b = bounce-average. Defining the matrix S_{ij} and the vector δS_j as:

$$S_{ij}(s,t) = \left\langle \int \mathrm{d}\vec{v} M_i M_j f_0 \right\rangle,\ \delta S_j(s,t) = \gamma_K \left\langle \int \mathrm{d}\vec{v} \delta f M_j \right\rangle, \qquad (3)$$

We solve the linear system $S_{ij} g_j = \delta S_i$ for the coeffs g_i and we have:

$$S_{\rm corr} = \sum_{i=1} g_i f_0 M_i \qquad (4)$$

Three purposes:

- Obtain a quasi-steady state: constant (time-averaged) values of fluxes, gradients, entropy
- Maintain the signal/noise ratio steady at high enough values
- Heat source (if kinetic energy conservation is disabled)

3. TCV equilibrium and profiles

Magnetic configuration: Ideal MHD equilibrium (CHEASE code)
TCV shot nr.43516, L-mode discharge
Radial coordinate $\rho_V = \sqrt{V(\psi)/V(\psi_a)}$, V = volume inside $\psi = \mathrm{const}$ surface.
Profiles
Flat profiles inside sawtooth inversion radius ($\rho_V < 0.5$), constant logarithmic gradients in the core ($0.5 < \rho_V < 0.8$), constant linear gradients in the **pedestal** region ($0.8 < \rho_V > 1.0$) [Sauter PoP 2014]

$$T(\rho_V) = \min\left(T_0, T_{\rm ped} \exp\left(-\kappa_T(\rho_V - \rho_{V,\rm ped})\right)\right) \quad \rho \le \rho_{V,\rm ped}$$
$$T_1(1 - \mu_T(\rho_V - \rho_{V,\rm edge})) \quad \rho_{V,\rm ped} < \rho \le \rho_{V,\rm edge} \qquad (5)$$

where T_0, T_1, $\rho_{V,\rm ped}$, $\rho_{V,\rm edge}$, κ_T and μ_T are given input parameters. Density profiles are defined in a similar way, with parameters n_0, n_1, κ_n and μ_n.
Normalized with $T_e(\rho_V = 1)$, $B_{\rm axis}$: c_{s0}, $\rho_{*0} = \rho_{s0}/a = 244.8$, $\chi_{GB0} = \rho_{s0} c_{s0} \rho_{*0}$

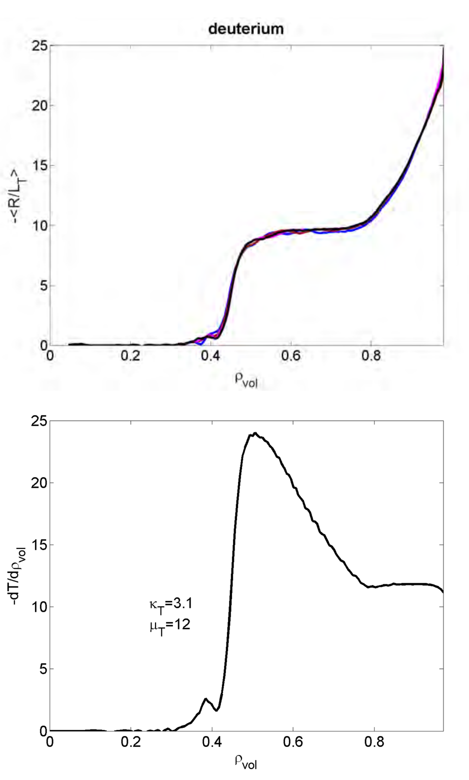

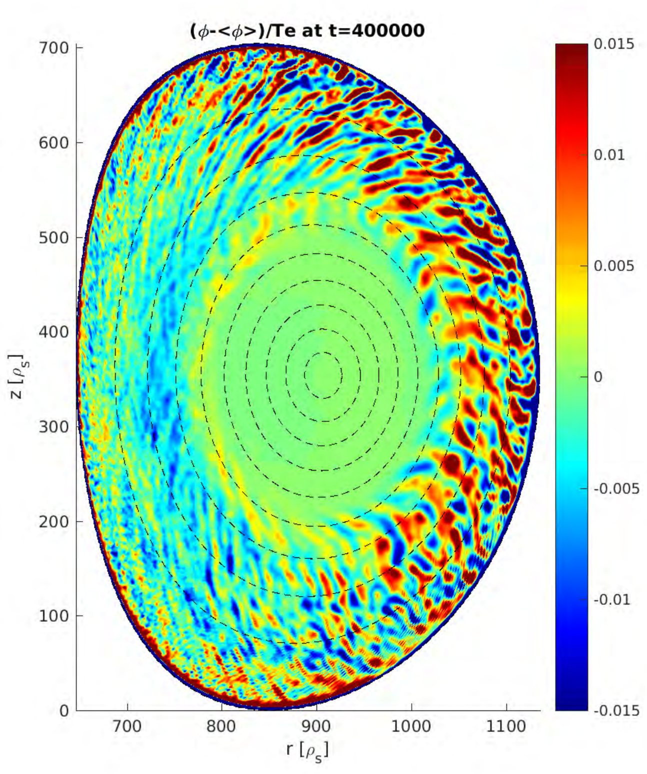

4. Effect of (non)-conserving sources on heat transport and flows

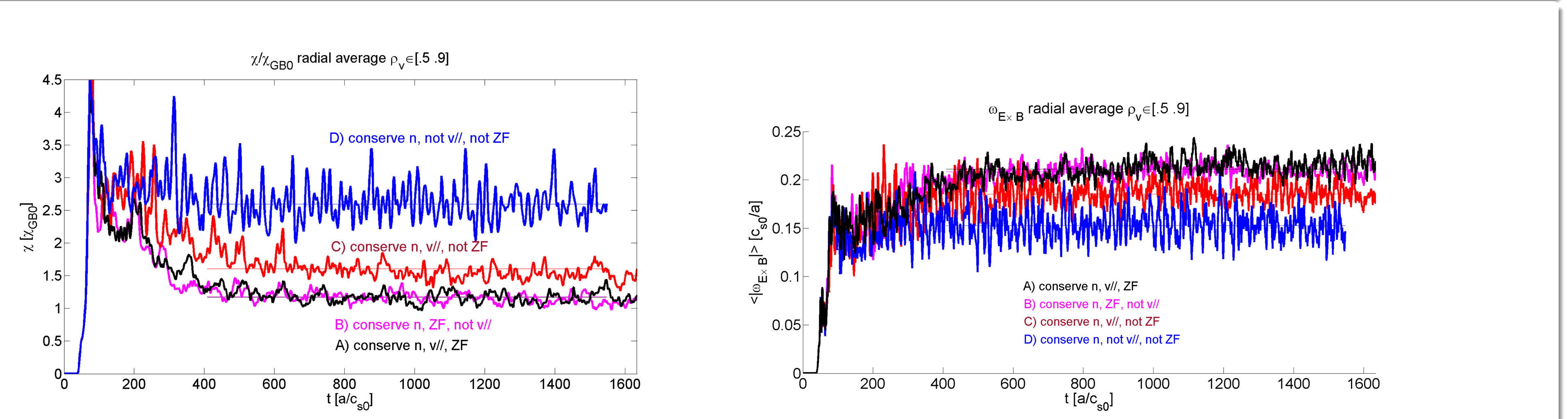

Figure 1: Effective ion heat diffusivity (left), $E \times B$ shearing rate (right) radially-avaeraged over $\rho_V \in [0.5, 0.9]$, vs time, for various $E \times B$ ZF and parallel flows conserving or non-conserving source operators.

Non conserving parallel flows alone: little effect on heat transport. Non-conserving $E \times B$ ZFs: 25% higher transport. *Non-conserving both $E \times B$ ZF and parallel flows leads to an overestimation of heat transport by a factor of more than 2. Higher transport is related to lower time-averaged $E \times B$ ZF shearing rates.*

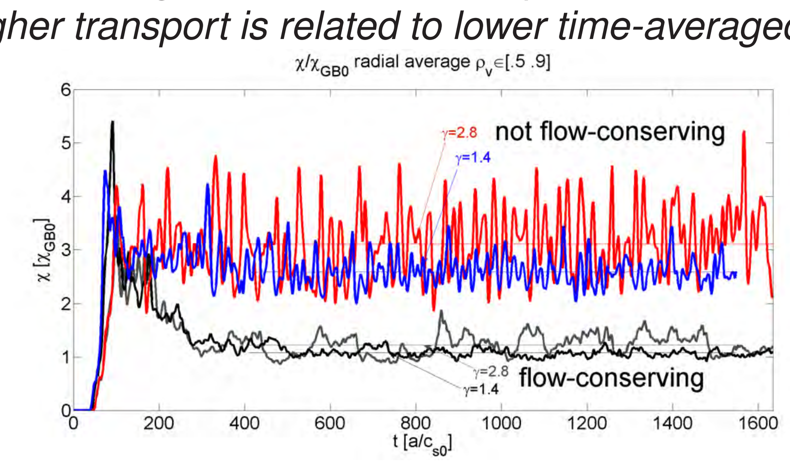

Figure 2: Effective ion heat diffusivity vs time for ZF- and $v_\parallel$-conserving (black, grey) and non-conserving (blue, red) sources.

Non-conserving ZF and parallel flows by the source leads to a (non-physical) $\sim$ 3.6 times enhanced sensitivity of the heat transport on the strength of the source operator. A factor 2 increase in $\gamma_K \rightarrow$ increase of χ by 0.14, which is within the uncertainty due to finite-time statistics, for the conserving case, but $\rightarrow$ increase of χ by 0.51, which is significant.

In more detail: effect of (non-)conservation on $v_\parallel$ and $E \times B$ ZF radial, time-averaged, profiles

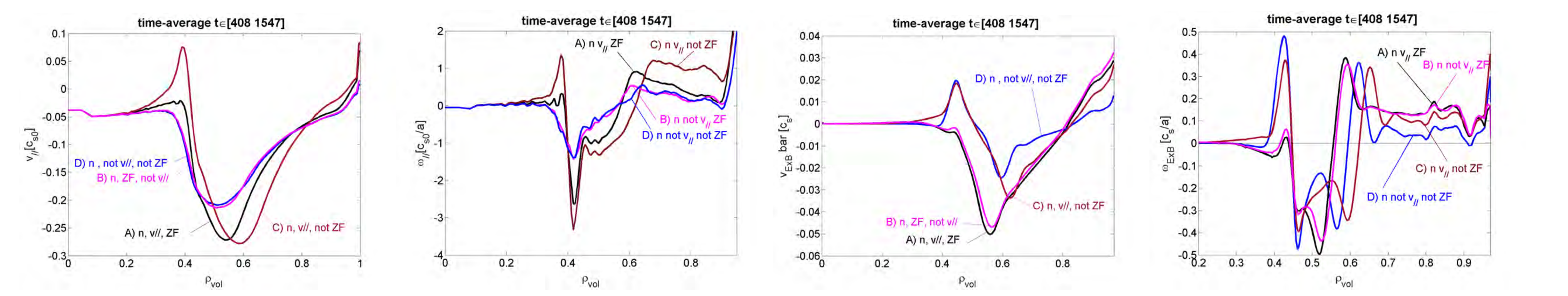

Interesting cross-effect of $v_\parallel$ and $E \times B$ ZF non-conservation: Non-ZF-conservation leads to a change in the parallel flow profile evolution.
Similarly, non-conservation of $v_\parallel$ leads to a marked decrease of the $E \times B$ ZF shearing rate in the region $0.6 < \rho_V < 0.95$.

5. GAM or not GAM, that is the question

TCV TPCI measurements: radially extended, coherent signal, $f \le f_{\rm GAM}$ [deMeijere PPCF 2014]

'Global GAM'? but theoretically a global GAM should propagate *above* the local GAM frequency, not below. So what is it?
The 'global feature' is also seen in global GK simulations [Vernay PhD 2012; Merlo PhD 2016; Villard Varenna 2014].

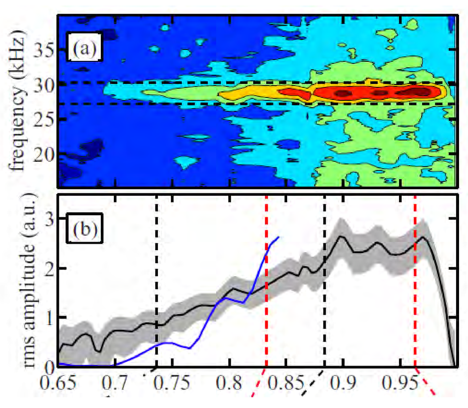

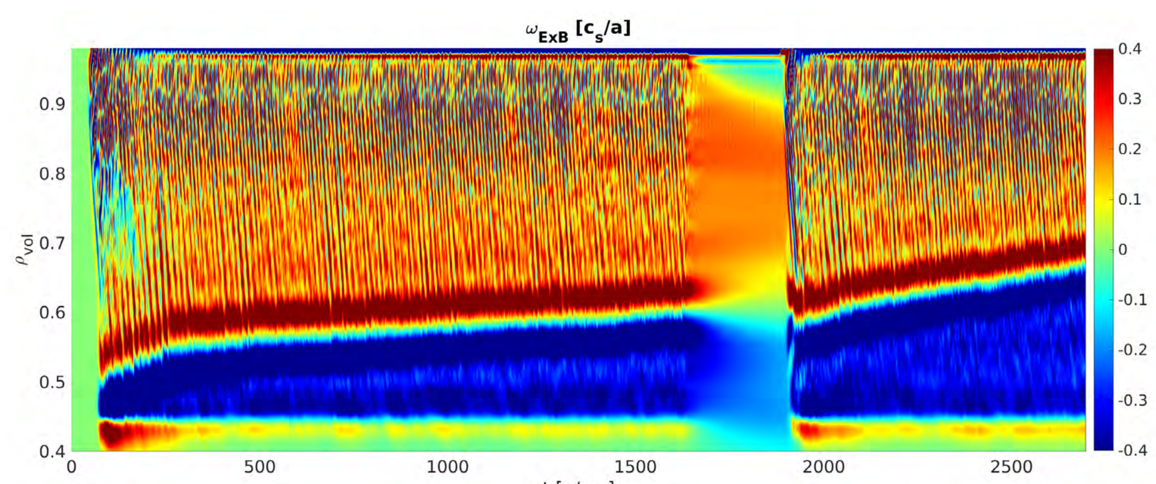

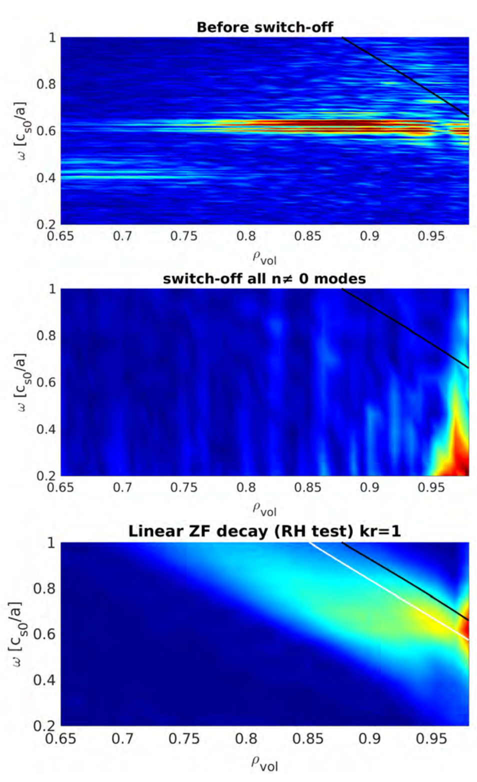

Artificially supressing all $n \neq 0$ modes at $t = 4 \times 10^5 \Omega_i^{-1} \rightarrow$ immediate disappearance of the regular oscillations. Restoring them at $t = 4.6 \times 10^5 \Omega_i^{-1} \rightarrow$ immediate reappearance. The signal after switch-off does not show any well-defined frequency. It is showing a very different response from the decay of an initial ZF (Rosenbluth-Hinton test)

Switch-off $n \neq 0$ **Linear ZF decay (RH test)**

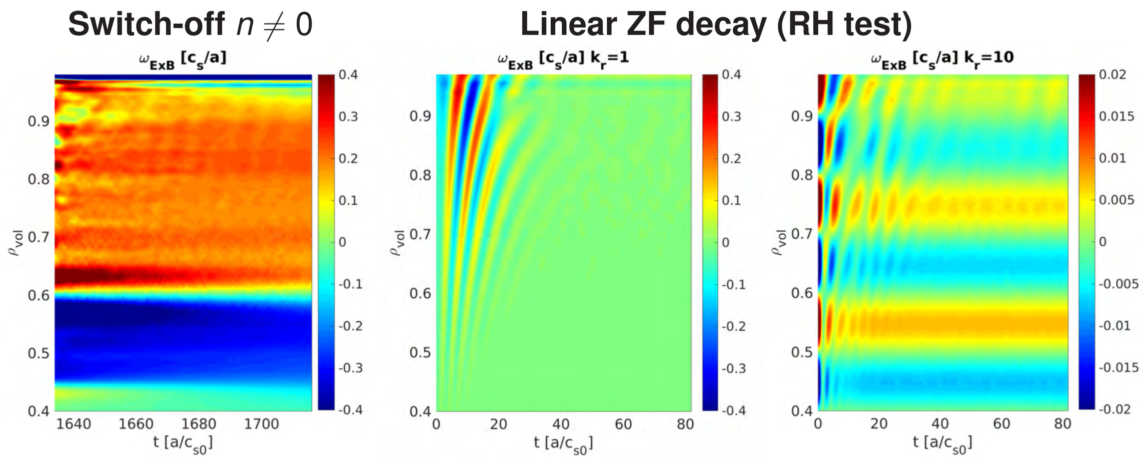

$\rightarrow$ **The global feature is a non-resonant excitation of avalanches by turbulence**

6. Effect of (non-)conserving sources on avalanches

Conserve n, $v_\parallel$, ZF | Conserve n, not $v_\parallel$, ZF | Conserve n, $v_\parallel$, not ZF | Conserve n, not $v_\parallel$, not ZF

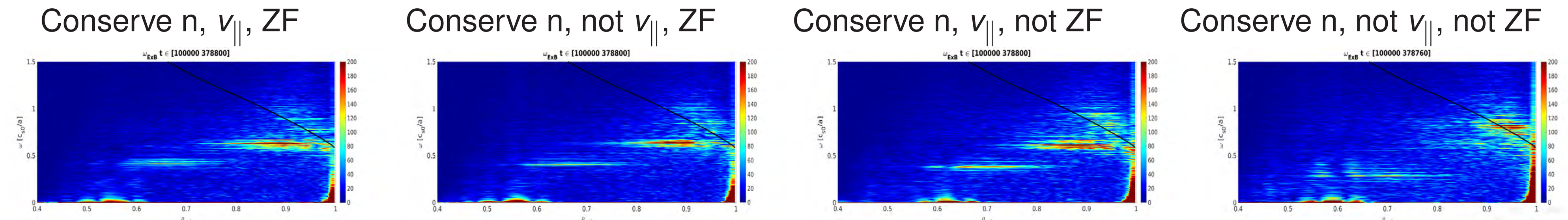

Using non-ZF-$v_\parallel$- conserving sources leads to the disappearance of the global feature.

$\rightarrow$ **Importance of keeping flow conservation in sources.**

Acknowledgements. *This work was partly supported by Eurofusion and by the Swiss National Science Foundation. Computations were performed on the PIZ DAINT platform at CSCS in Switzerland and on the HELIOS supercomputer at IFERC-CSC in Japan. We thank F. Jenko, A. Bottino, A. Biancalani, S. Coda, Z. Huang for stimulating discussions.*